Adsorptive Removal of Ciprofloxacin by Ferric Chloride Modified Biochar

Huaxuan Zhao [1,2], Zhengmei Cao [3], Jin Li [1,2], Yinhai Lang [1,2,*]
[1] College of Environmental Science and Engineering, Ocean University of China, Qingdao 266100, China;
[2] Key Laboratory of Marine Environmental Science and Ecology, Ministry of Education, Ocean University of China, Qingdao 266100, China;
[3] Qingdao Environmental Monitoring Central Station, Qingdao 266071, China.
Email: yhlang@ouc.edu.cn.

Key words: Ciprofloxacin, magnetic biochar, adsorption, mechanism

Abstract: A magnetic biochar (MBC) was fabricated through pyrolysis of $FeCl_3$ impregnated reed stalk powder, and used for ciprofloxacin (CIP) adsorption from aqueous solution. The structure and properties of the MBC were characterized by elemental analyzer, BET, SEM and FTIR. Results showed that the prepared MBC had a large specific surface area and pore volume, which was conducive to the CIP adsorption. Adsorption of CIP on MBC was of strong pH dependence and demonstrated a bimodal curve. Ionic strength increasing was advantageous to the CIP adsorption. The Langmuir model and the pseudo second-order model presented better fittings for the adsorption equilibrium and kinetic data. Adsorption thermodynamic parameters manifested that the adsorption behavior was a spontaneous, endothermic and entropy-increasing process. Pore-filling effect, π-π EDA interaction, electrostatic interaction, hydrogen bonding formation and hydrophobic interaction were important mechanisms for CIP adsorption on the MBC.

1 INTRODUCTION

Ciprofloxacin (CIP) is one of the quinolone antibiotics used to treat human and veterinary bacterial infection because of its strong, broad-spectrum antibacterial property and high mobility (Wang et al., 2016). Due to its incompletely metabolized by humans and domestic animals and released in effluent from drug manufacturing, CIP has become a widely monitored and frequently detected antibiotic in surface water, wastewater of the effluent treatment plants and hospitals (He et al., 2015; Giger et al., 2003; Rodriguez et al., 2015). Moreover, CIP in the environment could increase the antibiotic resistance of the living organisms and threaten human health (Berhane et al., 2016). Therefore, it is imperative to eliminate CIP from the water environments.

Adsorption method shows a promising prospect for the elimination of quinolone antibiotics. Magnetic biochar is an ideal adsorbent due to its abundant raw materials, versatility and particularly higher adsorption capacity for that the magnetization of carbonaceous material can create additional adsorption sites in comparison with the non-magnetic adsorbent (Reguyal et al., 2017). Moreover, magnetic biochar has been found to provide simple separation after treatment using a magnet (Thines et al., 2017). Compared with the other common separation technologies such as centrifugation and filtration, the magnetic separation method is more efficient and cost-effective (Shang et al., 2016).

These synthesized magnetic biochars have been used for adsorption removal of multiple contaminants, such as heavy metals, hydrophobic organic pollutants, dyestuffs, pharmaceuticals, entrophication anions such as nitrate and phosphate, from aqueous solutions (Mohan et al., 2014; Bastami and Entezari, 2012; Ma et al., 2015; Wang et al., 2017; Usman et al., 2016; Li et al., 2016). However, very few researches have been conducted with respect to the synthesis of magnetic biochar using reed biomass as raw material. Furthermore, the studies on the CIP adsorption behaviors were not enough.

In this task, a magnetic biochar (MBC) was prepared by one-step synthesis through pyrolysis of $FeCl_3$ impregnated reed stalk powder, and used for the CIP adsorption from aqueous solution. Batch

Zhao, H., Cao, Z., Li, J. and Lang, Y.
Adsorptive Removal of Ciprofloxacin by Ferric Chloride Modified Biochar.
In *Proceedings of the International Workshop on Environment and Geoscience (IWEG 2018)*, pages 56-61
ISBN: 978-989-758-342-1
Copyright © 2018 by SCITEPRESS – Science and Technology Publications, Lda. All rights reserved

adsorption experiments were employed to delve into the adsorption behaviors and mechanisms of CIP on MBC. The MBC served as a practical and effective adsorbent presented great potential in wastewater treatment.

2 MATERIALS AND METHODS

2.1 Preparation and Characteristics of MBC

The reed stalk powder (40 g) was immersed into the prepared $FeCl_3$ solution (40 g $FeCl_3 \cdot 6H_2O$ in 60 mL of ultrapure water) for 2 h and then dried under air. The obtained biomass was pyrolyzed at a temperature of 873.15 K for two hours in an oxygen-limited environment. After washed and dried overnight, the obtained magnetic biochar, denoted as MBC, was milled and sieved to pass through a 100-mesh sieve (<0.15 mm).

The elemental compositions (C, H, S, O and N) of the MBC were determined using an elemental analyzer. The microscopic features were characterized by SEM. The BET surface area and micropore volume were measured using a Physisorption and Chemisorption Analyzer. The amounts of the acidic oxygen-containing groups on the MBC surface were measured by the Boehm's titration method (Boehm, 1994). The surface functional groups of the MBC were determined by FTIR spectra in the 4000 to 400 cm^{-1} spectral range. The measurement of point of zero charge (pH_{pzc}) was on the basis of a reported paper (Bastami and Entezari, 2012).

2.2 Adsorption Experiments

All the adsorption experiments were conducted under the darkness condition in 150 mL Erlenmeyer flasks with 50 mL of CIP solutions and 50 mg of MBC samples in a reciprocating shaker at 190 $r \cdot min^{-1}$ and 298.15 K unless stated otherwise. Separate sets of experiments were carried out to examine the influences of pH and ionic strength on CIP adsorption. The pH values of CIP solutions (10 $mg \cdot L^{-1}$) were adjusted in the range of 4-12 with NaOH or HCl solutions. 10 $mg \cdot L^{-1}$ CIP solutions containing 0 to 1.0 $mol \cdot L^{-1}$ NaCl were prepared to investigate the effect of ionic strength. In the adsorption kinetic experiment, 10 $mg \cdot L^{-1}$ CIP solutions were used with adsorption time ranging from 0.5 to 24 h. The initial CIP concentrations were set from 2 to 20 $mg \cdot L^{-1}$ at 298.15, 308.15, 318.15 K for the adsorption isotherms study. All batch adsorption experiments were performed with three replicates. The CIP concentrations were analysed with a UV-visible spectrophotometer at 272 nm.

The adsorption capacity of the MBC was calculated by the following equation:

$$q_e = \frac{V(C_0 - C_e)}{m} \quad (1)$$

Where q_e ($mg \cdot g^{-1}$) is the amount of adsorbed CIP, C_0 and C_e ($mg \cdot L^{-1}$) are the initial and equilibrium CIP concentrations, respectively, V (L) is the solution volume, and m (g) is the MBC weight.

3 RESULTS AND DISCUSSION

3.1 Characterizations of MBC

The calculated weight percentage of iron accounted for 17.56% in MBC, indicating a lot of iron was successfully loaded on the surface of MBC. MBC had a relatively high porosity with BET surface area of 238.3 $m^2 \cdot g^{-1}$ and total pore volume of 0.257 $cm^3 \cdot g^{-1}$. The pH_{pzc} was 2.5 for MBC.

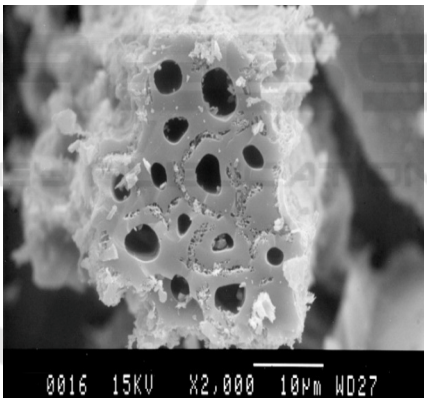

Figure 1: SEM image of the MBC.

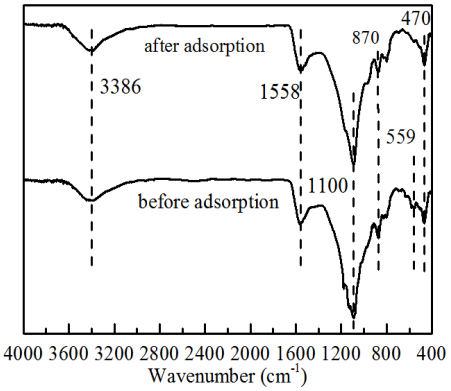

Figure 2: FTIR analysis spectra of the MBC.

Details about the structures and morphologies of the MBC were investigated using SEM analysis. Figure 1 showed that the MBC possessed roughness and pores within its structure. A good dispersion of particles with different shapes has been observed on the surface of the MBC, which clearly delineated the presence of iron oxide particles attached and dispersed onto the surface of MBC.

Figure 2 showed the FTIR spectra of MBC before and after CIP adsorption. The FTIR spectra indicated that the adsorption peak at 559 cm^{-1} can be corresponding to the Fe-O stretching vibration (Bastami and Entezari, 2012). After adsorption, the disappearance of this peak indicated that the Fe-O bond can serve as adsorption sites for CIP. The peaks of MBC at 3386, 1558, 1100 and 870 cm^{-1} can be attributed to the skeletal vibration of O-H, C=O or C=C, and C-O bonds, respectively (Bastami and Entezari, 2012 ; Zhou et al., 2017 ; Zhu et al., 2014). The above results indicated that there were many oxygen-contained functional groups on the MBC surface. The Boehm's test also indicated that many acidic oxygen-containing groups (such as carboxyl, lactone, phenolic hydroxyl and carbonyl) were on the MBC surface and the total amount of these groups was about 3.263 $mmol \cdot g^{-1}$. The oxygen-containing functional groups can provide adsorption sites for CIP, so that CIP formed hydrogen bonds with the groups on the MBC surface.

3.2 Effect of pH

The influence of pH on CIP adsorption coefficient [K_d, calculated by equation (2)] presented a bimodal curve in Figure 3. The K_d values for the adsorption of CIP on MBC reached its first maximum at pH 6. A further increase of pH up to 7.2 led to a decrease in K_d values. The second sharp peak was observed at pH 11 and then the K_d values decreased gradually up to pH 12.1.

$$K_d = \frac{q_e}{C_e} = \left(\frac{C_0 - C_e}{C_e}\right)\frac{V}{m} \quad (2)$$

CIP (pK_{a1}=6.1, pK_{a2}=8.7) can exist as cations (CIP^+), zwitterions ($CIP^{\pm}$) and anions (CIP^-) with the change of solution pH values. In addition, the pH_{pzc} of the MBC was at pH of 2.5. Therefore under the experimental conditions, the MBC surface was negatively charged. Accordingly, the first peak of the K_d value at pH 6 was due to the electrostatic attraction interaction between CIP^+ and the negatively charged MBC surface. When 6<pH<7.2, the electrostatic attraction interaction decreased, bringing about the decrease in CIP adsorption. The second peak of the K_d value at pH 11, where the final CIP solution pH after adsorption shifted to 8.2 because of proton release from MBC surface, was mainly attributed to the hydrophobic effect. The CIP solubility is lower in neutral solutions than in acidic or alkaline solutions (Jalil et al., 2015). A further increase of pH up to 12.1, the adsorption of CIP^- species declined on account of the electrostatic repulsion between negatively charged MBC surface and CIP^-. The same phenomenon was described when investigating sulfonamides adsorption on acidic functionalized biochar (Ahmed et al., 2017)

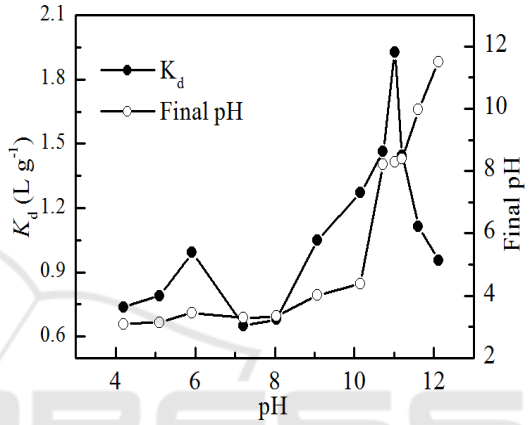

Figure 3: Effect of pH on CIP adsorption on MBC.

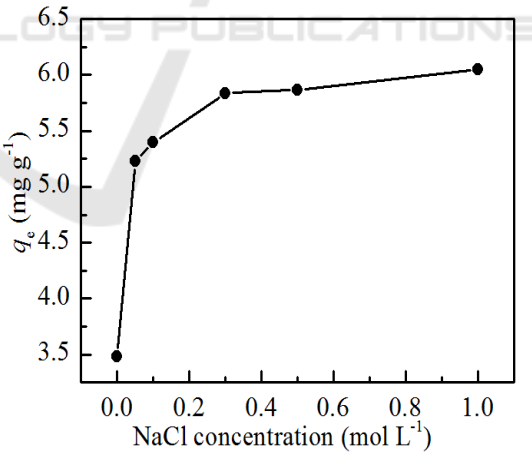

Figure 4: Effect of ionic strength on CIP adsorption on MBC.

3.3 Effect of Ionic Strength

As can be seen in Figure 4, the amounts of CIP adsorbed on MBC increased by 71.4% when the initial NaCl concentration increased from 0 to 1.0 $mol \cdot L^{-1}$. The salting out effect between CIP

molecules and NaCl may result in the decrease of CIP solubility in aqueous solution when NaCl was added, which facilitating the diffusion of more CIP molecules to the MBC surface and increasing the CIP adsorption amount (Peng et al., 2016).

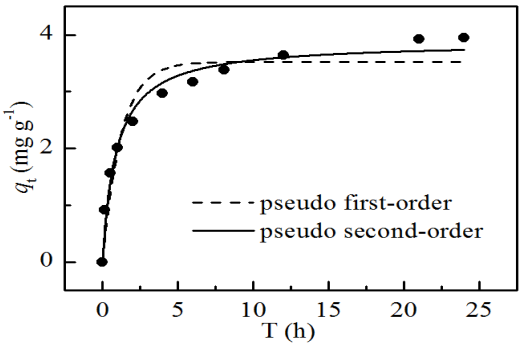

Figure 5: Adsorption kinetics of CIP on MBC.

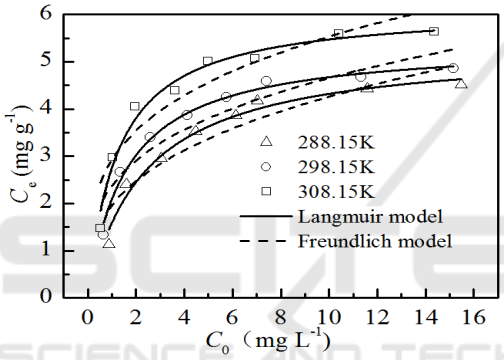

Figure 6: Adsorption isotherms of CIP on MBC.

3.4 Adsorption Kinetics

As illustrated in Figure 5, the adsorption rate was quite rapid in the first four hours and then slowed down progressively, bringing about the equilibrium state. There were plenty of active adsorption sites on the MBC surface. The adsorption rate decreased with the adsorption sites occupied (Mao et al., 2016). The result indicated that the saturation of CIP adsorption on MBC was obtained in approximately 24 h.

The plots of the pseudo first-order (PFO) and pseudo second-order (PSO) kinetic models for CIP adsorption onto the MBC were given in Figure 5. The PSO model provided the better fitting for the adsorption process compared with the PFO model. The determination coefficient (R^2) value of the PSO model (0.955) was higher than that of the PFO model (0.854). Futhermore, the value of $q_{e,exp}$ (4.11 mg·g^{-1}) was evidently closer to the predicted values calculated theoretically by the PSO model (3.97 mg·g^{-1}), manifesting that PSO model was more appropriate in describing the adsorption kinetic of CIP on the MBC (Zhu et al., 2014). The results manifested that chemisorption process was the rate-limiting step in the elimination of CIP by MBC (Jalil et al., 2015). This discovery was similar to the adsorption kinetic of tetracycline on magnetic porous biochar (Ahmed et al., 2017).

3.5 Adsorption Isotherms

In order to further investigate the adsorption mechanisms of CIP onto the MBC, the experimental data was fitted with Langmuir and Freundlich models as illustrated in Figure 6. The Langmuir models gave higher determination coefficient values (R^2=0.974, 0.985, 0.973) to describe the adsorption equilibrium data for CIP on MBC at 288.15, 298.15 and 308.15 K compared to Freundlich models, indicating the monolayer coverage of CIP on the MBC. Maximum Langmuir adsorption capacity (q_e) were 5.34, 5.41 and 6.14 mg·g^{-1} for CIP adsorption on MBC at 288.15, 298.15, 308.15 K, respectively.

For Langmuir isotherms, the values of k_L increased with increasing temperature, indicating the combining capacity for CIP on MBC increased gradually. When R_L values are between 0 and 1, the adsorption process is favorable. In this study, the R_L values were in the range of 0.058-0.105, indicating the favorability of CIP adsorption on MBC (Reguyal et al., 2017).

3.6 Adsorption Thermodynamics

The thermodynamic parameters (ΔG^0, ΔH^0, ΔS^0) for the adsorption process were calculated from the following equations and given in Table 1.

$$\Delta G^0 = -RT \ln K_d \quad (3)$$

$$\Delta G^0 = \Delta H^0 - T\Delta S^0 \quad (4)$$

Where T (K) is the absolute temperature, R (8.314 J·mol^{-1}·K^{-1}) is the universal gas constant.

Table 1: Thermodynamic parameters of CIP adsorption on MBC.

Temperature (K)	K_d (L g^{-1})	ΔG^0 (kJ mol^{-1})	ΔH^0 (kJ mol^{-1})	ΔS^0 (J mol^{-1} K)
288.15	0.402	-0.915	24.616	88.602
298.15	0.685	-1.801		
308.15	1.070	-2.687		

ΔH^0 was positive, suggesting that the adsorption process was an endothermic process. The positive

value of ΔS^0 demonstrated the randomness-increasing character of the adsorption of CIP on MBC. The negative ΔG^0 indicated the feasibility and spontaneous nature of the adsorption of CIP onto the MBC surface. The adsorption behavior was a spontaneous, endothermic and entropy-increasing process. In addition, the absolute values $|\Delta G^0|$ were less than 20 kJ·mol^{-1}, revealing that a physical adsorption may be included in the reaction processes (Feng et al., 2013). This also suggested that pore-filling effect may be a significant mechanism for the CIP adsorption on account of the abundant pores within the MBC structure (Deng et al., 2017).

3.7 Adsorption Mechanisms

The mechanisms of CIP adsorption on MBC may be attributed to a combination of pore-filling effect, π-π EDA interaction, hydrogen bonding formation, electrostatic interaction and hydrophobic interaction.

The pore-filling effect played a significant role in the adsorption of CIP on MBC. The rich porosity of the MBC played a crucial role in the elimination of CIP. Chun et al reported that the surface and pore properties of biochars were the main factors influencing the adsorption of hydrophobic organic pollutants and concluded that the pore-filling effect was a predominant mechanism (Chun et al., 2004). Wang et al also found the pore-filling effect promoted the norfloxacin adsorption on magnetic biochars tremendously (Wang et al., 2017).

FTIR analysis indicated that the MBC surface was enriched with –OH, –COOH and aromatic groups. –OH and –COOH on the MBC surface could form hydrogen bonding with N-containing and F-containing groups on the CIP molecules. The aromatic groups acting as strong electron donors can interact with CIP molecules which had a strong π-electron acceptor nature to form a π-π bond according to the π-π EDA theory (Wang et al., 2017; Ahmed et al., 2017).

Among interactions, electrostatic interaction was also an important factor for CIP adsorption on the MBC. It can be confirmed by the former discussion. And the hydrophobicity significantly affected the CIP adsorption due to the decreased solubility.

4 CONCLUSIONS

MBC with a relatively high porosity was prepared for the elimination of CIP from aqueous solution. Adsorption of CIP on MBC was of strong pH dependence and presented a bimodal curve. Ionic strength increasing was advantageous to the CIP adsorption. The Langmuir model and the pseudo second-order kinetic model presented better fittings for the adsorption equilibrium and kinetic data, respectively. The adsorption behavior was a spontaneous, endothermic and entropy-increasing process. The adsorption of CIP on MBC was controlled by multiple mechanisms. MBC is a good adsorbent for CIP adsorption.

ACKNOWLEDGMENT

This study was sponsored by the Natural Science Fundation of Shandong Province (ZR2016EEM28).

REFERENCES

Ahmed M B, Zhou J L, Ngo H H, et al 2017 Single and competitive sorption properties and mechanism of functionalized biochar for removing sulfonamide antibiotics from water[J] *Chemical Engineering Journal* **311** 348.

Bastami T R, Entezari M H 2012 Activated carbon from carrot dross combined with magnetite nanoparticles for the efficient removal of p-nitrophenol from aqueous solution[J] *Chemical engineering journal* **210** 510.

Berhane T M, Levy J, Krekeler M P S, et al 2016 Adsorption of bisphenol A and ciprofloxacin by palygorskite-montmorillonite: Effect of granule size, solution chemistry and temperature[J] *Applied Clay Science* **132** 518.

Boehm H P 1994 Some aspects of the surface chemistry of carbon blacks and other carbons[J] *Carbon* **32(5)** 759.

Chun Y, Sheng G, Chiou C T, et al 2004 Compositions and sorptive properties of crop residue-derived chars[J] *Environmental science & technology* **38(17)** 4649.

Deng H, Feng D, He J, et al 2017 Influence of biochar amendments to soil on the mobility of atrazine using sorption-desorption and soil thin-layer chromatography[J] *Ecological Engineering* **99** 381.

Feng Y, Dionysiou D D, Wu Y, et al 2013 Adsorption of dyestuff from aqueous solutions through oxalic acid-modified swede rape straw: adsorption process and disposal methodology of depleted bioadsorbents[J] *Bioresource technology* **138** 191.

Giger W, Alder A C, Golet E M, et al 2003 Occurrence and fate of antibiotics as trace contaminants in wastewaters, sewage sludges, and surface waters[J] *CHIMIA International Journal for Chemistry* **57(9)** 485.

He K, Soares A D, Adejumo H, et al 2015 Detection of a wide variety of human and veterinary fluoroquinolone antibiotics in municipal wastewater and wastewater-impacted surface water[J] *Journal of pharmaceutical and biomedical analysis* **106** 136.

Jalil M E R, Baschini M, Sapag K 2015 Influence of pH and antibiotic solubility on the removal of ciprofloxacin from aqueous media using montmorillonite[J] *Applied Clay Science* **114** 69.

Li R, Wang J J, Zhou B, et al 2016 Recovery of phosphate from aqueous solution by magnesium oxide decorated magnetic biochar and its potential as phosphate-based fertilizer substitute[J] *Bioresource technology* **215** 209.

Ma H, Li J B, Liu W W, et al 2015 Novel synthesis of a versatile magnetic adsorbent derived from corncob for dye removal[J] *Bioresource technology* **190** 13.

Mao H, Wang S, Lin J Y, et al 2016 Modification of a magnetic carbon composite for ciprofloxacin adsorption[J] *Journal of Environmental Sciences* **49** 179.

Mohan D, Kumar H, Sarswat A, et al 2014 Cadmium and lead remediation using magnetic oak wood and oak bark fast pyrolysis bio-chars[J] *Chemical Engineering Journal* **236** 513.

Peng P, Lang Y H, Wang X M 2016 Adsorption behavior and mechanism of pentachlorophenol on reed biochars: pH effect, pyrolysis temperature, hydrochloric acid treatment and isotherms[J] *Ecological Engineering* **90** 225.

Reguyal F, Sarmah A K, Gao W 2017 Synthesis of magnetic biochar from pine sawdust via oxidative hydrolysis of FeCl2 for the removal sulfamethoxazole from aqueous solution[J] *Journal of Hazardous Materials* **321** 868.

Rodriguez-Mozaz S, Chamorro S, Marti E, et al 2015 Occurrence of antibiotics and antibiotic resistance genes in hospital and urban wastewaters and their impact on the receiving river[J] *Water research* **69** 234.

Shang J, Pi J, Zong M, et al 2016 Chromium removal using magnetic biochar derived from herb-residue[J] *Journal of the Taiwan Institute of Chemical Engineers* **68** 289.

Thines K R, Abdullah E C, Mubarak N M, et al 2017 Synthesis of magnetic biochar from agricultural waste biomass to enhancing route for waste water and polymer application: A review[J] *Renewable and Sustainable Energy Reviews* **67** 257.

Usman A R A, Ahmad M, El-Mahrouky M, et al 2016 Chemically modified biochar produced from conocarpus waste increases NO3 removal from aqueous solutions[J] *Environmental geochemistry and health* **38(2)** 511.

Wang B, Jiang Y, Li F, et al 2017 Preparation of biochar by simultaneous carbonization, magnetization and activation for norfloxacin removal in water[J] *Bioresource Technology* **233** 159.

Wang F, Yang B, Wang H, et al 2016 Removal of ciprofloxacin from aqueous solution by a magnetic chitosan grafted graphene oxide composite[J] *Journal of Molecular Liquids* **222** 188

Zhou Z, Liu Y, Liu S, et al 2017 Sorption performance and mechanisms of arsenic (V) removal by magnetic gelatin-modified biochar[J] *Chemical Engineering Journal* **314** 223.

Zhu X, Liu Y, Qian F, et al 2014 Preparation of magnetic porous carbon from waste hydrochar by simultaneous activation and magnetization for tetracycline removal[J] *Bioresource technology* **154** 209.

SCITEPRESS SCIENCE AND TECHNOLOGY PUBLICATIONS